

Magnetic Properties of Bulk and Thin Nd₂Fe₁₄B Films after Corrosion Action

V. CONSTANTIN^a, E.I. NEACȘU^a, A.M. POPESCU^a, A. GALYAS^b, O. DEMIDENKO^{b,*}
AND K. YANUSHKEVICH^b

^a“Ilie Murgulescu” Institute of Physical Chemistry of the Romanian Academy,
Splaiul Independentei 202, Bucharest, Romania

^bScientific-Practical Materials Research Center NAS, P. Brovki Str. 19, Minsk, Belarus

The corrosion action for bulk and thin Nd₂Fe₁₄B films magnets in different corrosion media was studied. The thin Nd-Fe-B films of $100 \text{ nm} \leq d \leq 1000 \text{ nm}$ were deposited on glass substrate by “flash” evaporation method. The structure and microstructure of the samples were studied by X-ray diffraction analysis, scanning electron microscopy. The temperature dependence of the magnetization before and after corrosion action was carried out by ponderomotive method in the temperature range $80 \leq T \leq 800 \text{ K}$. It is shown that the specific magnetizations of the thin Nd-Fe-B films with $d \geq 1000 \text{ nm}$ are comparable to those measured for the powder samples. The values of the coercive and saturation fields were determined from the hysteresis loops measurements.

DOI: [10.12693/APhysPolA.127.368](https://doi.org/10.12693/APhysPolA.127.368)

PACS: 61.05.cp, 75.50.Bb, 75.50.Vv, 75.70.-i

1. Introduction

During the last years, the using of sintered NdFeB magnets in large motor and generator applications has become more common. The remanence of NdFeB material is superior in comparison to other types of magnet materials. Thin films based on NdFeB permanent magnets also are studied in the recent years, due to the fundamental interest [1–10] and due to their potentially applications in magnetic recording devices [11–14]. Actual is the problem of corrosion protection of based on NdFeB products in bulk and film states.

The aim of presented work is to investigate macromagnetic properties of bulk and thin Nd-Fe-B layers prepared onto glass substrate after corrosive action.

2. Experimental

A commercially available MQP-B powder product was used as a precursor. Thin Nd₂Fe₁₄B layers were deposited by thermal evaporation (flash method) in a standard sputtering equipment UHV-71R-2 type on the glass substrates. A special device on the basis of shock vibration for a strictly dosed spilling powder charge into the evaporation zone was applied. During deposition the powder grains fall on the tantalum evaporator, heated to a temperature significantly above the melting point of the evaporated material ($\approx 2500 \text{ }^\circ\text{C}$). Rapid evaporation and subsequent cooling of the sample maintains its composition and structure.

The crystal structure of the as-deposited alloy thin films was characterized by X-ray diffraction (XRD) using

an X-ray diffractometer (model DRON-2, Russia) with Cu K_α -radiation. X-ray pictures were obtained by automatic recording of reflection intensities with 0.03° scanning step and 2–3 s exposition per step.

The morphology of the obtained thin films was analyzed before and after the corrosion process by scanning electron microscopy (SEM) using “Philips XL-30-SEM” equipped with an energy dispersive X-ray spectrometer (EDS). The accuracy of the measurements for the used equipment was about $\pm 0.1 \text{ wt}\%$.

The investigations of the specific magnetization for the bulk and thin Nd-Fe-B films were carried out by ponderomotive method in a magnetic field of 0.86 T in the temperature range of $80\text{--}1100 \text{ K}$ [15].

The corrosion behavior of NdFeB thin films was investigated by open circuit potential (OCP) and anodic polarization curves (linear and Tafel) using a potentiostat/galvanostat Princeton-PARSTAT 2273 (with a specialized soft “Power Corr”) in a $3.5 \text{ wt}\%$ NaCl aerated solution at a temperature of $25 \pm 2 \text{ }^\circ\text{C}$. The electrochemical measurements were performed in a glass cell of 50 ml capacity with thermostated jacket, with a conventional three electrodes: Ag/AgCl (with KCl 0.3 M) as the reference electrode and a platinum plate as counter electrode, both of them of Radiometer production. Each working electrodes had 1 cm^2 of exposed surface.

3. Results and discussion

The X-ray analysis of the bulk permanent magnets samples and powders obtained by crushing the magnets themselves, showed that their crystal structure is almost identical. It corresponds to the tetragonal $R42/mnm$ space group of Nd₂Fe₁₄B compound [16]. X-ray patterns of the thin films with the thickness of $\approx 1000 \text{ nm}$ indicate the presence of a free iron. With decreasing thickness of layers in the observed X-ray patterns one

*corresponding author; e-mail: orion_misk@tut.by

can see diffuse reflections of the “halo” type instead of a large number of distinct reflections of the tetragonal structure for the $\text{Nd}_2\text{Fe}_{14}\text{B}$ powder. This experiment revealed the significant amorphous structure with decreasing film thickness.

X-ray photoelectron spectroscopy analysis of the thin film was used to determine the chemical states of the elements present on the surface. The high resolution photoelectron spectra of the most significant XPS transitions (C 1s, O 1s, Fe 2p, Nd 3d, and B 1s) were recorded for the as-prepared and sputtering samples (1 min, 2 min).

The presence of C 1s peak on the XPS spectra is due to environmental contamination or handling of the samples. It was already shown that the peaks of Fe and Nd can be found in the spectrum NdFeB of the Nd-rich phase [17]. On the surface of the analyzed samples the key elements (Nd, Fe, B) are oxidized (Nd_2O_3 , Fe_2O_3 , B_2O_3) except boron which is found also as borate.

SEM images for the thin film samples with the magnitude of $500\times$ and $2000\times$ show the existence of discontinuities like little holes. EDS analysis shows only the peaks corresponding to Fe, Nd and O. The peaks observed for C and Si are originating from the glass substrate.

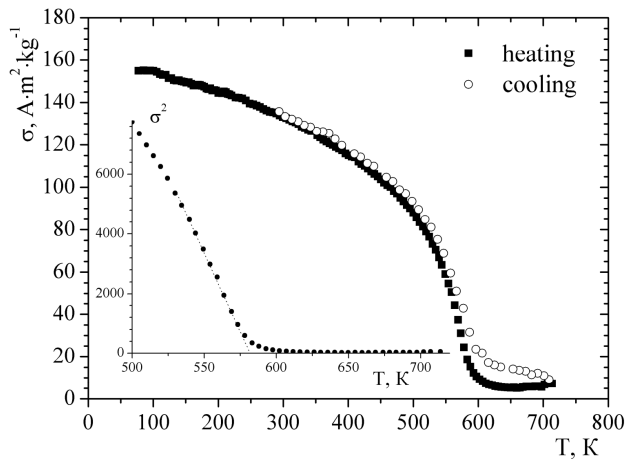


Fig. 1. Temperature dependence of specific magnetization for $\text{Nd}_2\text{Fe}_{14}\text{B}$ initial powder before corrosion action.

From temperature dependence of the specific magnetization for the initial Nd–Fe–B powder (Fig. 1) it follows that the specific magnetization of the sample at 100 K exceeds $150 \text{ A m}^2 \text{ kg}^{-1}$. The temperature dependence of the specific magnetization during the cooling process shows that the heating of the sample to 720 K does not reduce the value of the specific magnetization. The Curie temperature of these alloys, determined from the $\sigma^2 = f(T)$ dependence is equal to $T_c = 570 \text{ K}$ (inset in Fig. 1). Analysis of $\sigma = f(T)$ for Nd–Fe–B alloy in the range of 600–720 K indicates that prolonged exposure of the $\text{Nd}_2\text{Fe}_{14}\text{B}$ powder at high temperatures can lead to partial precipitation of iron and, consequently, disruption of the chemical composition of the alloy. The temperature dependence of the specific

magnetization $\sigma = f(T)$ of oxidation products in the surface of $\text{Nd}_2\text{Fe}_{14}\text{B}$ permanent magnet (Fig. 2) exhibit anomalies indicating the existence of at least three magnetic phases with different transition temperatures to the paramagnetic state: $T_c^1 \approx 600 \text{ K}$, $T_c^2 \approx 830 \text{ K}$, $T_c^3 \approx 1040 \text{ K}$. Analyzing the temperature dependence of the specific magnetization for different stoichiometric compositions of $\text{Nd}_2\text{Fe}_{14}\text{B}$, Fe_3O_4 and pure Fe, we can conclude that these components determine the magnetic properties of the samples after corrosive action.

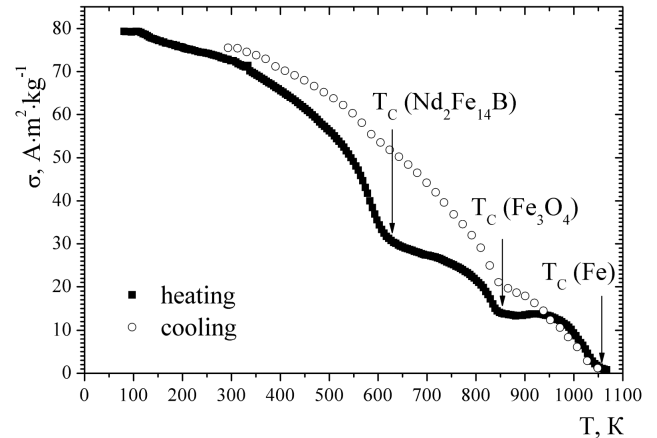


Fig. 2. Temperature dependence of specific magnetization for $\text{Nd}_2\text{Fe}_{14}\text{B}$ initial powder after corrosion action.

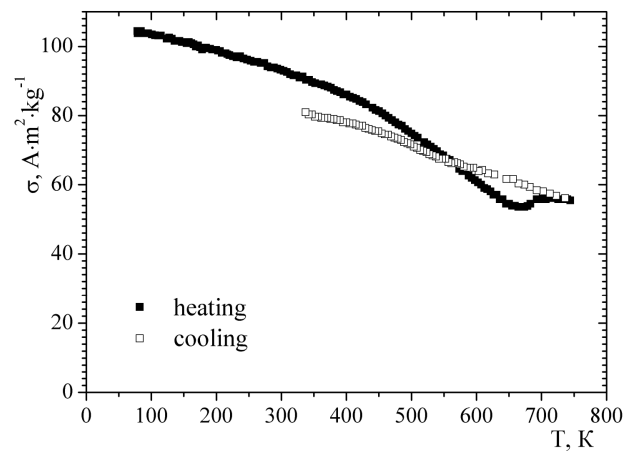


Fig. 3. Temperature dependence of specific magnetization for $\text{Nd}_2\text{Fe}_{14}\text{B}$ thin film with $d > 100 \text{ nm}$ before corrosion action.

Figure 3 presents the temperature dependence of the specific magnetization for Nd–Fe–B film with $d > 100 \text{ nm}$. Measurements showed that the specific magnetization value in such layers decreases to about $\approx 105 \text{ A m}^2 \text{ kg}^{-1}$ at 100 K. During the cooling, the $\sigma = f(T)$ dependence indicates significant reduction of the specific magnetization. Such a behavior evidently proves partial decomposition of the alloy.

After exposure to oxidation processes the specific magnetization and transition temperature to the paramagnetic state increase (Fig. 4) up to $150 \text{ A m}^2 \text{ kg}^{-1}$ and $840\text{--}1010 \text{ K}$, respectively. This is probably due to the intensive formation of Fe_3O_4 in the surface layer of the Nd–Fe–B thin films. The transition temperature to the paramagnetic state for Fe_3O_4 is in the range of $T_C \approx 820\text{--}860 \text{ K}$ and for iron — $T_C \approx 1040 \text{ K}$. Therefore, the release of these ions from the thin Nd–Fe–B layers may increase the specific magnetization.

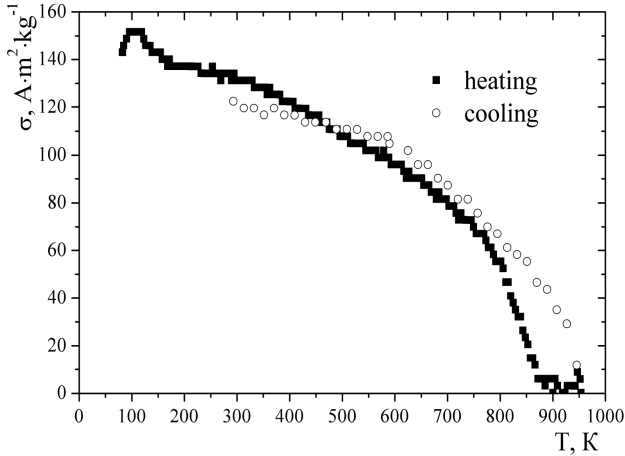


Fig. 4. Temperature dependence of specific magnetization for $\text{Nd}_2\text{Fe}_{14}\text{B}$ thin film with $d > 100 \text{ nm}$ after corrosion action.

4. Conclusions

The method for depositing thin $\text{Nd}_2\text{Fe}_{14}\text{B}$ films onto glass substrate is developed. The X-ray diffraction study confirmed the presence of the tetragonal $R42/mnm$ space group structure in the thin films, in accordance with results observed for the $\text{Nd}_2\text{Fe}_{14}\text{B}$ polycrystalline powder. After corrosion action performed for the bulk and thin $\text{Nd}_2\text{Fe}_{14}\text{B}$ films we have observed elements such as $\text{Nd}_2\text{Fe}_{14}\text{B}$, Fe_3O_4 and pure Fe.

Acknowledgments

This research was financed by Romanian Academy and Belarus Academy of Science bilateral project 2011–2013 No. F12RA-007 and “EU(ERDF)-Romanian Government” that allowed for acquisition of the research infrastructure under POS-CEEO2.2.1 INFRANANOCHEM project No. 19/01.03.2009.

References

- [1] W. Tang, Z.Q. Jin, J.-R. Zhang, G. Gu, J.-M. Li, Y.-W. Du, *J. Magn. Magn. Mater.* **185**, 241 (1998).
- [2] S.N. Piramanayagam, M. Matsumoto, A. Morisako, S. Takei, *IEEE Trans. Magn.* **33**, 3643 (1997).
- [3] H. Homburg, Th. Sinnemann, S. Methfessel, M. Rosenberg, B.X. Gu, *J. Magn. Magn. Mater.* **83**, 231 (1990).
- [4] H. Lemke, T. Lang, T. Goddenhenrich, C. Heiden, *J. Magn. Magn. Mater.* **148**, 426 (1995).
- [5] M. Yu, Y. Liu, S.H. Lion, D.J. Sellmyer, *J. Appl. Phys.* **83**, 6611 (1998).
- [6] D.J. Keavney, E.E. Fullerton, J.E. Pearson, S.D. Bader, *IEEE Trans. Magn.* **32**, 4440 (1996).
- [7] H. Lemke, C. Echer, G. Thomas, *IEEE Trans. Magn.* **32**, 4404 (1996).
- [8] F.J. Cadieu, T.D. Cheung, L. Wickramasekara, N. Kamprath, *IEEE Trans. Magn.* **22**, 752 (1986).
- [9] K.D. Aylesworth, D.J. Sellmyer, G.C. Hadjipanayis, *J. Magn. Magn. Mater.* **98**, 65 (1991).
- [10] A.J.M. Geursten, J.C.S. Kools, L. de Wit, J.C. Lodder, *Appl. Surf. Sci.* **96-98**, 887 (1996).
- [11] D.J. Mapps, R. Chandrasekhar, K. O’Grady, J. Cambridge, A. Petford Long, R. Doole, *IEEE Trans. Magn.* **33**, 3007 (1997).
- [12] J.F. Zasadzinski, C.U. Segre, E.D. Rippert, *J. Appl. Phys.* **61**, 4278 (1987).
- [13] S. Yamashita, J. Yamasaki, M. Ikeda, N. Iwabuchi, *J. Appl. Phys.* **70**, 6627 (1991).
- [14] Ya.L. Linetsky, N.V. Kornilov, *J. Mater. Eng. Perform.* **4**, 188 (1995).
- [15] K.I. Yanushkevich, *Methods of specific magnetization and magnetic susceptibility measurement*, Assurance system of measurement uniformity of the Republic of Belarus, MVI. MN 3128-2009, BelSIM, Minsk 2009.
- [16] International Centre for Diffraction Data, PCPDFWIN, 1998, Vol. 2, No. 88-2285, No. 89-3632.
- [17] S. Mao, H. Yang, Z. Song, J. Li, H. Ying, K. Sun, *Corr. Sci.* **53**, 1887 (2011).